ARCHIVES OF ELECTRICAL ENGINEERING VOL. 59(1-2), pp. 99-107 (2010)

DOI 10.2478/s10171-010-0008-x

# Induction motor analysis employing optimal torque predictor and massive conductor approach

**JAKUB BERNAT, SŁAWOMIR STĘPIEŃ**

*Chair of Computer Engineering, Poznań University of Technology*
*ul. Piotrowo 3a, 60-965 Poznań, Poland*
*tel. +48(061) 6652504*
*e-mail: Jakub.Bernat@put.poznan.pl, Slawomir.Stepien@put.poznan.pl*

(Received: 25.05.2010, revised: 10.06.2010)

**Abstract:**This research presents a method for the simulation of the magneto-mechanical system dynamics taking motion and eddy currents into account. The major contribution of this work leans on the coupling the field-motion problem considering windings as the current forced massive conductors, modelling of the rotor motion composed of two conductive materials and the torque calculation employing the special optimal predictor combined with the modified Maxwell stress tensor method. The 3D model of the device is analysed by the time stepping finite element method. Mechanical motion of the rotor is determined by solving the second order motion equation. Both magnetic and mechanical equations are coupled in the iterative solving process. Presented method is verified by solving the TEAM Workshop Problem 30.

**Key words:** finite element method, eddy current, torque, prediction

## 1. Introduction

In the modern computational electromagnetics the force problem is still an issue. The method of the computation we can chose from the collection of publications and handbooks [5-7]. In analysis of the field-motion problems, the force or the torque computing plays the special role, because it is the coupling quantity in the magneto-mechanical model described by the field and mechanical equations [2-4, 8].

The accuracy of the force computation is related to the discretisation, motion techniques etc. Hence, one may notice, that the force computation is always corrupted by the numerical noises or imperfections. It has an impact on the force prediction error [7].

The use of the Maxwell's stress tensor technique combined with the optimal predictor that reduces the torque computation error is described in this article. The method supported by the prediction technique permits an effective computation of the global torque, minimising the uncertainty related to the choose of the integration surface around the rotor.

Employing the AC induction motor problem presented by Prof. Kent Davey (TEAM Workshop Problem 30 – Fig. 1) [1], the author shows the usefulness of the proposed methodology.

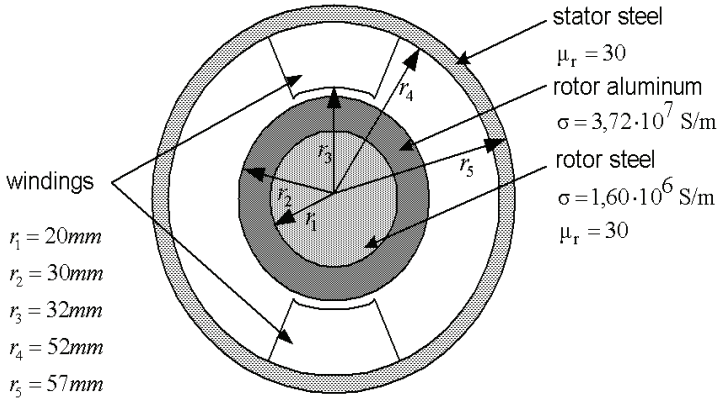


Fig.1. Single phase induction motor problem

For the purpose, the time-stepping finite element analysis of the electromagnetic field considering the motor windings as massive conductors [9] and the time-stepping model of the mechanical motion considering the optimal torque predictor [10] is presented.

## 2. The field model

The model of the device is described by the magnetic vector potential **A** and the electric scalar potential $V$ [9]. The problem is defined in three regions: $\mathbf{\Omega}_c^i$ – region of immovable conductor, $\mathbf{\Omega}_c^m$ – region of movable conductor and $\mathbf{\Omega}_n$ – non-conducting region.

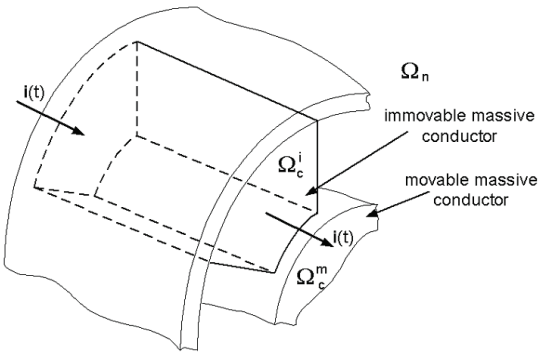


Fig. 2. Model of the induction motor part

The total current $i(t)$ is injected by the boundary surfaces of the immovable massive conductor. In the time stepping 3D FE model, the input is the stator phase current. The equations that describe the electromagnetic field are written in the cylindrical coordinate

that describe the electromagnetic field are written in the cylindrical coordinate system for 27 node elements with linear shape functions [9]. The rotor part of the mesh is rotated at each iteration step by the angle determined from the motion differential equation.

The governing equations of the electromagnetic field are represented by Maxwell's equations and consider the eddy current problem in the massive windings [9]:

$$\nabla \times \left( \frac{1}{\mu} \nabla \times \mathbf{A} \right) + \left( \sigma \frac{\partial \mathbf{A}}{\partial t} + \sigma \nabla V - \sigma \mathbf{v} \times \left( \nabla \times \mathbf{A} \right) \right) = 0 \,. \tag{1}$$

In conducting regions additionally is performed [9]:

$$-\nabla \cdot \left( \sigma \frac{\partial \mathbf{A}}{\partial t} + \sigma \nabla V - \sigma \mathbf{v} \times \left( \nabla \times \mathbf{A} \right) \right) = 0 \;\; \text{in } \Omega_c \,, \tag{2}$$

where $\mathbf{v} = \boldsymbol{\omega} \times \mathbf{r}$ represents the speed of the rotor. The current prescribed on each phase winding is defined on the surface placed on the boundary of the analyzed system.

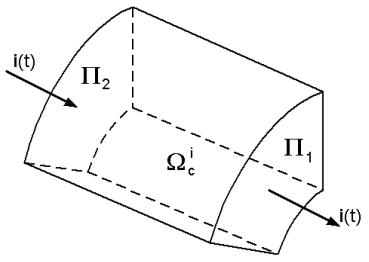


Fig. 3. Model of a massive winding

As shown in the Fig. 3, the total current $i(t)$ is injected to the massive conductor by the boundary surface $\Pi_1$ and rejected by $\Pi_2$. Hence, for the single phase system, the prescribed currents may be defined as follows:

$$\int_{\Pi_1} \sigma \left( \frac{\partial \mathbf{A}}{\partial t} + \nabla V \right) \mathbf{d\Pi} = i(t) \;\text{ on }\; \mathbf{\Pi}_1 \,, \tag{3}$$

$$\int_{\Pi_2} \sigma \left( \frac{\partial \mathbf{A}}{\partial t} + \nabla V \right) \mathbf{d\Pi} = -i(t) \;\text{ on }\; \mathbf{\Pi}_2 \,. \tag{4}$$

This approach is very comfortable, because the difficult and arduous problem related to the stranded coil wind in the complex mesh may be simplified. Of course, this model is useful for the low frequency analysis. It considers eddy currents in the conductor. The analysis with higher frequencies may produce a special case of the eddy current problem, namely skin effect.

In presented model, windings are considered as the multi-conducting system. The solution of the field equations refer to (1) – (2) is obtained by minimizing the corresponding energy

functional. The minimization is performed by means of the FEM using the first-order cylindrical elements. This is the weighted residual method for which the weighted functions are the same as the shape functions. The approach is used to derive the following matrix equation [9]:

$$\begin{bmatrix} \mathbf{C}+\dfrac{\mathbf{D}}{\Delta t} & \mathbf{F}_1 & \mathbf{H}_1 & \cdots & \mathbf{H}_4 \\ \mathbf{F}_2 & \mathbf{G}\cdot\Delta t & \mathbf{K}_1\cdot\Delta t & \cdots & \mathbf{K}_4\cdot\Delta t \\ \mathbf{H}_1^T & \mathbf{K}_1^T\cdot\Delta t & m_1\cdot\Delta t & \cdots & 0 \\ \vdots & \vdots & \vdots & \ddots & \vdots \\ \mathbf{H}_4^T & \mathbf{K}_4^T\cdot\Delta t & 0 & \cdots & m_4\cdot\Delta t \end{bmatrix} \begin{bmatrix} \mathbf{A}(t+\Delta t) \\ \mathbf{V}(t+\Delta t) \\ V^1(t+\Delta t) \\ \vdots \\ V^4(t+\Delta t) \end{bmatrix} = \begin{bmatrix} -\dfrac{\mathbf{D}}{\Delta t}\mathbf{A}(t) \\ \mathbf{F}_2^T\mathbf{A}(t) \\ i^1(t)\cdot\Delta t+\mathbf{H}_1^T\mathbf{A}(t) \\ \vdots \\ i^4(t)\cdot\Delta t+\mathbf{H}_4^T\mathbf{A}(t) \end{bmatrix}, \tag{5}$$

where **C** is the nonsymmetrical matrix related to the magnetic field and the induced currents from movement, **D** is the diagonal matrix related to the induced currents from the field change, **F** represents matrices related to the static and induced electric field, **G** is the matrix related to the static electric field. Rows $\mathbf{H}_j^T$ and $\mathbf{K}_j^T$ for $j = 1,..,4$ are related to the definition of prescribed currents on the boundary surfaces refer to (3)-(4). Each conductivity $m_j$ is obtained as the sum of each row $\mathbf{K}^T$. The unknown vector consists of the vector of the magnetic vector potentials **A**, vector of the electric scalar potentials defined inside the analysed area **V** and unknown scalar potentials $V^j$ defined on the boundary surfaces of the massive conductors (Fig. 3). Presented system of the field equations (5) is non-symmetric and solved by the bi-conjugate gradient algorithm (BiCG).

## 3. The torque prediction and motion model

The electromagnetic torque is calculated via the Maxwell stress tensor MST [6]. The global force is calculated along a surface in the airgap around the rotor. The torque is obtained from the relationship

$$\mathbf{T} = \oint_{S(\Omega_c^m)} (\mathbf{r}\times\mathbf{P})\,dS\,, \tag{6}$$

where $\mathbf{r} = [r, 0, 0]$ is a radius vector that connects origin of the co-ordinate system to the surface $S$ placed around the rotor region $\mathbf{\Omega}_c^m$. The vector $\mathbf{P} = [0, P_\varphi, 0]$ denotes the stress.

The global torque is determined from the combination of the surface stresses produced by the electromagnetic field. In case of the presented problem, the $z$ – component of the torque is calculated by the relationship [6]:

$$T \approx r\sum_{l} P_l \Delta S_l = r\sum_{l} H_{\varphi,l} B_{r,l} \Delta S_l \,, \tag{7}$$

and is evaluated along the optimal surface placed in the airgap between the rotor and the immovable massive conductor.

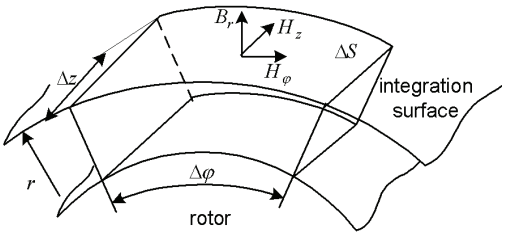


Fig. 4. The surface part around the rotor

In case of the solution of the mechanical motion, the prediction of the torque $T$ is introduced. In this paper the optimization of the torque prediction is related to the computation for the different integration surfaces, that are important for the accuracy of the torque defined in (6). The surface which ensures the best accuracy is chosen. The torque obtained in (7) can be corrupted by the numerical noises and imperfections. Thus, the technique which is able to obtain the filtered and smooth curve of the torque is necessary [10].

For this reason, let us assume, that the calculated torque is corrupted with an error $e$. The average value of the $e$ is assumed to be zero, the variance is assumed to be $\lambda^2$ and is the model uncertainty. Moreover let us assume, that the error $e$ and time $t$ are independent. Let us consider the model with the exogenous input

$$T(t+\Delta t) \approx aT(t) + ce(t) + e(t+\Delta t)\,, \tag{8}$$

where $a$ is known and $c$ is a scaling factor [10]. When calculate the expectation from the difference of the calculated torque $T$ (via the Maxwell stress tensor method) and its any prediction $T^*$

$$\begin{aligned} E\left[T(t+\Delta t) - T^*(t+\Delta t)\right]^2 &= E\left[aT(t) + ce(t) - T^*(t+\Delta t)\right]^2 + \\ + E\left[e(t+\Delta t)\right]^2 &= E\left[aT(t) + ce(t) - T^*(t+\Delta t)\right]^2 + \lambda^2 \geq \lambda^2 \end{aligned}\,, \tag{9}$$

then it is visible, that the variance of the prediction error is constrained by the $\lambda^2$. Taking above into account, we may proof that the optimal predictor $\hat{T}$ should minimise the expectation

$$\min E\left[T(t+\Delta t) - T^*(t+\Delta t)\right]^2, \tag{10}$$

for

$$e(t) = T(t) - \hat{T}(t)\,. \tag{11}$$

The optimal torque predictor is

$$\hat{T}(t+\Delta t) \approx aT(t) + ce(t) = aT(t) + cT(t) - c\hat{T}(t) = -c\hat{T}(t) + (c+a)T(t), \tag{12}$$

where: $T$ is the input torque obtained from the Maxwell Stress calculations and $\hat{T}$ is the torque predictor. It is easy to calculate that the prediction error does not depend on the coefficient $c$ which makes possibility to control the uncertainty influence on the torque prediction.

The described mechanism is used to obtain the global torque for the distributed parameters approach. It means that the prediction method is employed for each sub-torque obtained during discretisation. This way, the global torque is the sum for all $n$ elements, that lies on the surface placed in the airgap

$$\hat{T}(t+\Delta t) \approx \sum_{l=1}^{n} \hat{T}_l(t+\Delta t). \tag{13}$$

In the case of the dynamic studies of the problem, the following matrix form as the state space description of the prediction is coupled with the field and motion models

$$\begin{bmatrix} \hat{T}_1(t+\Delta t) \\ \vdots \\ \hat{T}_l(t+\Delta t) \\ \vdots \\ \hat{T}_n(t+\Delta t) \end{bmatrix} = - \begin{bmatrix} c_{11} & \cdots & c_{1l} & \cdots & c_{1n} \\ \vdots & \ddots & \vdots & & \vdots \\ c_{l1} & \cdots & c_{ll} & \cdots & c_{\mathrm{ln}} \\ \vdots & & \vdots & \ddots & \vdots \\ c_{n1} & \cdots & c_{nl} & \cdots & c_{nn} \end{bmatrix} \begin{bmatrix} \hat{T}_1(t) \\ \vdots \\ \hat{T}_l(t) \\ \vdots \\ \hat{T}_n(t) \end{bmatrix} + \tag{14}$$

$$+ \begin{bmatrix} a_{11}+c_{11} & \cdots & a_{1l}+c_{1l} & \cdots & a_{1n}+c_{1n} \\ \vdots & \ddots & \vdots & & \vdots \\ a_{l1}+c_{l1} & \cdots & a_{ll}+c_{ll} & \cdots & a_{\mathrm{ln}}+c_{\mathrm{ln}} \\ \vdots & & \vdots & \ddots & \vdots \\ a_{n1}+c_{n1} & \cdots & a_{nl}+c_{nl} & \cdots & a_{nn}+c_{nn} \end{bmatrix} \begin{bmatrix} T_1(t) \\ \vdots \\ T_l(t) \\ \vdots \\ T_n(t) \end{bmatrix}.$$

The angular speed and rotor displacement are evaluated by solution of the rotational motion equation

$$J\frac{d\omega}{dt} = \hat{T}. \tag{15}$$

The $J$ is a moment of the rotor inertia, $\omega$ is the angular speed and $\hat{T}$ represents the optimal prediction of the rotor torque. The discrete rotor speed and displacement are determined using the backward Euler's approximation for the motion equation

$$\begin{bmatrix} 1 & -\Delta t \\ 0 & 1 \end{bmatrix} \begin{bmatrix} \Theta(t+\Delta t) \\ \omega(t+\Delta t) \end{bmatrix} = \begin{bmatrix} \Theta(t) \\ \omega(t) + \Delta t \frac{1}{J} \hat{T}(t+\Delta t) \end{bmatrix}. \tag{16}$$

The motion in the electromagnetic field is realized using the fixed grid technique. In this approach the grid of the discretisation is independent of the rotor position. The moving body displacement may be updated at each iteration step. This approach enables to avoid of the stability loss during solution of field equations (5).

## 4. Numerical experiment

To demonstrate the effectiveness of the method, the single phase induction motor has been tested. The motor geometry and its excitation are detailed in the description of the TEAM Problem 30 [1]. This paper examines problem in which the eddy currents in the rotor composed of two different materials and are induced by the time harmonic current on the massive windings and the rotation of the rotor. The massive conductors are excited by the current 2045.175 A at 60 Hz. The rotor is made from the aluminum and the steel. For the experiment purpose, the following densities are assumed 2700 kgm$^{-3}$ and 7800 kgm$^{-3}$, respectively.

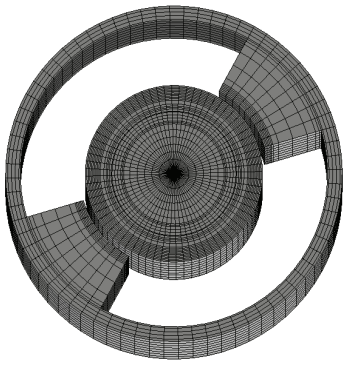

Fig. 5. The mesh of analyzed motor

The presented device is axisymmetric, therefore to run the rotor, the motor has been tested with the initial torque $\hat{T}(0) = 0.1$Nm. The size of the vector of the partial predictors is 360 and each eigenvalue of the matrix composed of $c$ elements defined in (14) is equal $\lambda_c = 0.99$. It ensures the stability of the prediction process.

To investigate the dynamic speed and torque characteristics, simulations are considered for the different size of the integration radius. There are compared the mean square errors $MSE = 1/q \sum_{k=1}^{q} \left(T_m - \hat{T}\right)^2$ with results given in [1], where $q$ is the number of the torque points $T_m$ presented in [1] and $\hat{T}$ is the torque estimate.

Figure 6 shows the error of the presented torque computation method due to the choosing of the integration radius. Thanks to the employed technique considering the torque uncertainty the change of the MSE is only about 15%.

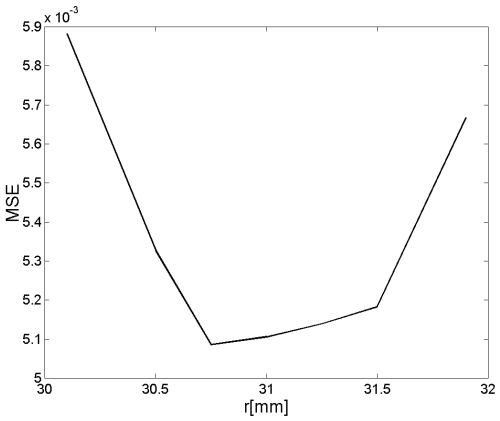


Fig. 6. MSE for different size of the integration radius

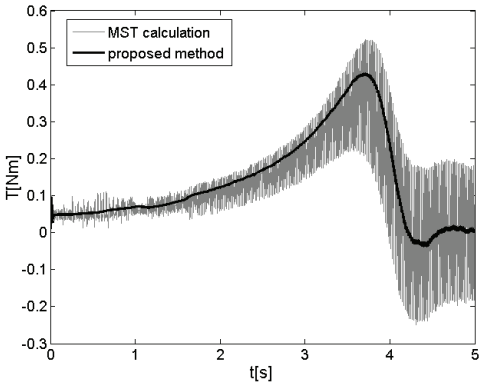


Fig. 7. Torque profile for $r = 30.75$ mm

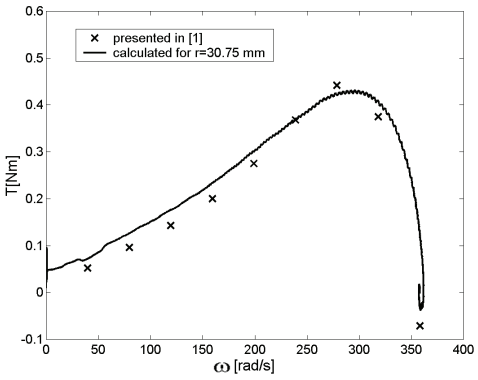


Fig. 8. Comparison of the torque-speed relationship

Figure 7 shows the temporary torque response obtained by the standard Maxwell stress tensor method for the "best" integration radius. The torque response calculated by the proposed method is also presented. The calculated torque is free of the redundant oscillations and expresses the required torque profile.

Figure 8 shows the torque-speed curve obtained from the proposed computations in comparison with the solution presented in the paper [1]. The comparison shows a quite good agreement.

For the illustration, the best solution of the problem, in which the torque response obtained from the Maxwell stress tensor and the torque obtained from the improved approach employing (14) are presented and compared in Fig. 8.

## 5. Conclusion

The method of analysis of the AC motor including the massive conductors approach and the optimal torque predictor is presented. The technique may be useful for the analysis of the dynamic characteristics of the electrical machines, where during the torque or the force computation may exist many uncertainties, for example related to the choosing of the optimal integration radius or the mesh imperfections.

As presented, the Maxwell stress tensor method without any prediction technique may produce oscillations or strong torque ripples due to the method of the motion approximation, for instance. Employing proposed prediction technique, these problems may be avoided.

Presented comparison of the torque calculated due to the proposed method and obtained analytically in [1] shows a quite good agreement.

## References

[1] K. Davey, *Analytic Analysis of Single- and Three Phase Induction Motors*. IEEE Trans. Mag. 34(5): 3721-3727 (1998).

[2] A. Demenko, D. Stachowiak, *Orthogonal transformation of moving grid model into fixed grid model in the finite element analysis of induction machines*. COMPEL 23(4): 1015-1022 (2004).

[3] H. De Gersem and K. Hameyer, *Finite element simulation of a magnetic brake with a soft magnetic solid iron rotor.* COMPEL 21(2): 296-306 (2002).

[4] G. Jang, J. Chang, D. Hong, K. Kim, *Finite element analysis of an electromechanical field of a BLDC motor considering speed control and mechanical flexibility*. IEEE Trans. Mag. 38(2): 945-948 (2002).

[5] D.H. Kim, D.A. Lowther, J.K. Sykulski, *Efficient Force Calculations Based on Continuum Sensitivity Analysis*. IEEE Trans. on Mag. 41(5): 1404-1407 (2005).

[6] G. Henneberger, P. Sattler, D. Shen, *Nature of the equivalent magnetizing current for the force calculation*. IEEE Trans. on Mag. 28(2): 1068-1071 (1992).

[7] F. Henrotte, *Handbook for the computation of electromagnetic forces in a continuos media.* ICS Newsletter 11(2): 10-17 (2004).

[8] A. de Oliveira, R. Antunes, P. Kuo-Peng, N. Sadowski, P. Dular, *Electrical machine analysis considering field-circuit-movement and skewing effects*. COMPEL 23(4): 1080-1091 (2004).

[9] A. Patecki, G. Szymański, S. Stępień, *Power losses analysis in the windings of electromagnetic gear.* COMPEL 23(3): 748-757 (2004).

[10] P. Stoica, A. Nehorai, *On the unequeness of prediction error models for systems with noisy input – output data*. Automatica 23: 541-543 (1987).